ARTICLES

Separation between Fast and Slow Polarizations in Continuum Solvation Models

Maurizio Cossi* and Vincenzo Barone

Dipartimento di Chimica, Università Federico II, via Mezzocannone 4, I-80134 Napoli, Italy

Received: March 15, 2000; In Final Form: August 9, 2000

Nonequilibrium solvation is important to describe many chemical processes in solution such as, for example, reactions involving light atoms or solvatochromic effects on UV spectra. This paper reports on an effective and general procedure to perform nonequilibrium calculations using continuum solvent models. First, "fast" dielectric constants are defined for the different processes which take place in solution (depending on their characteristic times), second, such constants are used in a new approach to separate fast and slow solvation components, and finally this approach is inserted in the framework of apparent surface charge (ASC) models. This procedure is applied to some test cases, involving very fast solute transitions which require the treatment of nonequilibrium effects.

1. Introduction

Solvation models based on the picture of the solvent as a polarizable continuum have been greatly enhanced in recent years:[1−4] now they are used[5−18] to compute molecular energies, electronic properties, energy gradients, and force constants in solution at the molecular mechanics, semiempirical, and ab initio Hatree−Fock (HF) and density functional (DF) levels. The most recent improvements allow the computation of energies and gradients at the MP2 level,[19] and the study of excited electronic states in solution using configuration interaction (CI), time-dependent HF and DF theory, and multi-configurational SCF (MC-SCF):[20] this last approach also provides excited state geometry optimizations in the presence of the solvent.

Now, a challenging task is to extend the continuum description of solvation effects from *static* to *dynamic* events: among the numerous interesting processes that would require a dynamical treatment of solvation, one can mention electron transfer reactions, photon absorption and emission, reactions involving the transfer of light atoms, molecular vibrations in solution, and geometry relaxation following an electronic transition.

From another point of view, solvent can play a crucial role in many chemical processes by providing "random forces" on reactant atoms or conversely by damping molecular motions due to friction effects. Sometimes it has been proposed to introduce one or more "solvation coordinates", in addition to the usual internal coordinates of the reactive system.[21,22] To afford these descriptions, one has to deal with nonequilibrium solvation effects appearing when the solvent polarization, or a part of it, deviates from the solute−solvent equilibrium characteristic of the static behavior.[23]

This article reports on a compact and unified treatment of nonequilibrium solvation in the framework of continuum solvent models,[1] among which the polarizable continuum model (PCM)[24] is one of the most flexible and powerful. The PCM formalism has been extensively discussed elsewhere,[12,15,16,25] and we shall recall only a few results here. Nonequilibrium PCM equations have been derived occasionally,[26−30] but always limited to some of the different PCM approaches, and sometimes with conflicting conclusions: here we shall present a new and effective treatment, valid for all the PCM versions with perfectly equivalent results.

We have mentioned the interest of nonequilibrium solvation for the study of solvatochromic effects, i.e., the solvent influence on electronic absorption and emission spectra: since the first works of Lippert, Ooshika, Bayliss, and McRae,[31−34] most of the nonequilibrium models have been proposed to treat this kind of problem. The approach we want to develop can be directly applied to the study of solvatochromic effects as well as to the other dynamical processes cited above.

In many applications, two sources of the solvent polarization are considered, having very different relaxation times:[35−44] one component of the solvent polarization is expected to relax at the same speed as electronic motions, and it is considered always equilibrated to the solute, while the other one remains fixed during electronic transitions and relaxes with the time scale typical of nuclear motions. The faster component is usually attributed to the solvent electronic polarizability (and it is sometimes referred to as optical, electronic, or noninertial), while the slower component is due to atomic (vibrational) relaxation and to molecular reorientations in the solvent (and it is called orientational, nuclear, or inertial).

However, a more careful analysis shows that the experimental behavior of most liquids subject to external oscillating fields (with frequency ω) is better described in terms of three distinct regimes, each one characterized by typical dielectric constants.[21,45] When ω is zero, or very small, the dielectric response is completely equilibrated to the external perturbation, and it is described by the static dielectric constant, ϵ. Another regime is reached when the external field oscillates in the microwave−far infrared region: here the liquid molecules are no longer able to reorient following the perturbation, and the dielectric response

* Corresponding author. E-mail: Mau@lsdm.dichi.unina.it.

10.1021/jp000997s CCC: $19.00
Published on Web 11/01/2000

TABLE 1: Atomic−Electronic and Purely Electronic Dielectric Constants for Some Liquids (*n* Extrapolated to Infinite Frequency)[45]

	T (°C)	ϵ_∞	n^2
chlorobenzene	20	2.36	2.24
tetrahydrofuran	20	2.20	1.95
water	25	4.2	1.75

is due to atomic and electronic polarizations only. In this case the proper dielectric constant is often called ϵ_∞ (though the involved frequencies are not "infinite" at all): for polar solvents ϵ_∞ is usually much smaller than ϵ. Finally, when higher frequencies are involved, only the electronic polarization remains in equilibrium, and the dielectric response is ruled by $\epsilon_{opt} = n^2$, where n is the refractive index at frequency ω. For many pure liquids and liquid mixtures $\epsilon_\infty \sim n^2$ (thus indicating that the atomic polarization plays a minor role), but in some cases the difference between ϵ_∞ and n^2 is not negligible at all (in Table 1) three illustrative examples are reported): note that in the literature these two notations are sometimes confused, and ϵ_∞ is used instead of n^2 to indicate the purely electronic dielectric constant.

The transition from the static to the atomic−electronic regimes (ϵ to ϵ_∞) has been carefully studied by many experimentalists. The phenomenological theory of dielectric relaxation explains the observed trends fairly:[45] if the orientational polariation is composed by one or more components, each relaxing exponentially with characteristic times $\{\tau_k, k = 1, 2, ...\}$, the overall dielectric response is ruled by a complex frequency dependent dielectric constant:

$$\hat{\epsilon}(\omega) = \epsilon_\infty + (\epsilon - \epsilon_\infty) \sum_k \frac{g_k}{1 + i\omega\tau_k} \tag{1}$$

with $\sum_k g_k = 1$. By applying the proper boundary conditions, eq 1 becomes

$$\hat{\epsilon}(\omega) = \epsilon_\infty + \frac{(\epsilon - \epsilon_\infty)}{1 + i\omega\tau} \tag{2}$$

in the case of a single relaxation process

$$\hat{\epsilon}(\omega) = \epsilon_\infty + \frac{(\epsilon - \epsilon_1)}{1 + i\omega\tau_1} + \frac{(\epsilon_1 - \epsilon_\infty)}{1 + i\omega\tau_2} \tag{3}$$

when two relaxation processes exist (the first leading to an intermediate dielectric constant ϵ_1, the second leading from ϵ_1 to ϵ_∞), and so on. We recall that ϵ_∞ is the dielectric constant observed when only atomic and electronic polarizations are fast enough to follow the perturbation.

A large body of experimental data provides this theory with quantitative parameters for most solvents of chemical interest. For example, water at 25 °C is well described[46] by a single relaxation process with $\epsilon = 78.4$, $\epsilon_\infty = 4.2$, and $\tau = 9 \times 10^{-12}$ s, while *n*-butyl alcohol at 155.8 K exhibits[47] two processes with $\epsilon = 49.1$, $\epsilon_1 = 4.4$, $\epsilon_\infty = 3.1$ and $\tau_1 = 31.2 \times 10^{-6}$ s, $\tau_2 = 0.08 \times 10^{-6}$ s: in Figure 1 the real part of $\hat{\epsilon}$ for these two liquids is reported as a function of ω.

In order to apply this approach to chemical reactions, a frequency ω must be associated to each of the dynamical processes we want to study in solution. Then we shall use two dielectric constants: the static constant ϵ, expressing the unperturbed solute−solvent equilibrium, and the fast constant $\epsilon_f(\omega)$ ruling the part of solvation which remains in equilibrium when the solute undergoes the process of frequency ω. When

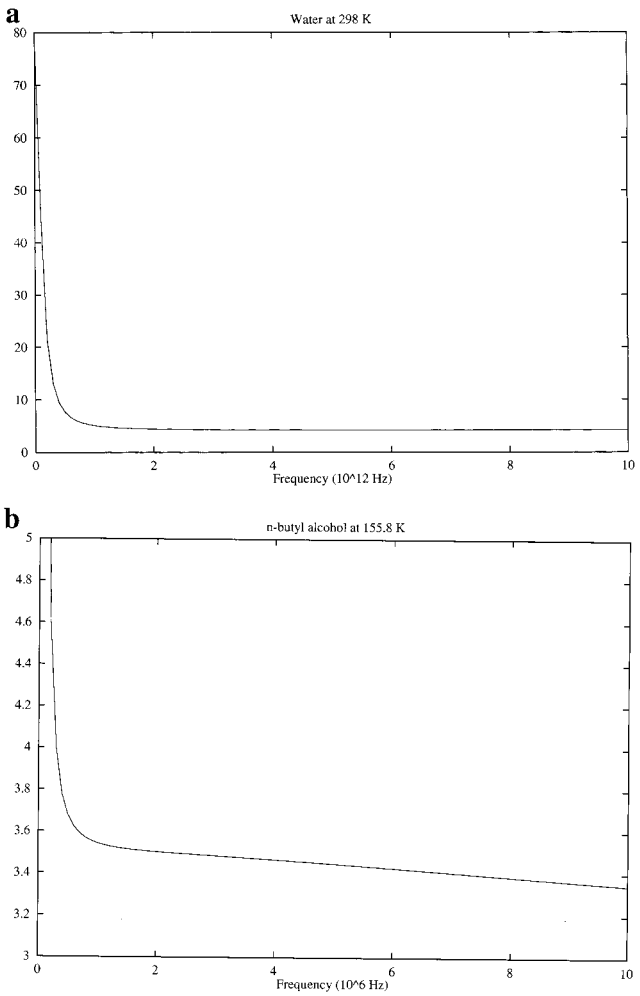

Figure 1. Real part of the frequency-dependent dielectric constant for water at 298 K (a) and *n*-butyl alcohol at 155.8 K (b). Note the different *x*-axis scales.

electronic state transitions are involved, as in the study of solvatochromic effects, ω is of the order of 10^4 cm^{-1} $\simeq 10^{14}$ s^{-1}: in this case the assumption $\epsilon_f = n^2$, usually made in this kind of study, is well justified. When slower solute perturbations are considered, such as atom displacements, we resort to eq 1: in this case, the fraction of the solvent polarization which is in equilibrium with the solute is determined by the real part of

$$\hat{\epsilon}: \ \epsilon_f(\omega) = R(\hat{\epsilon}) = \epsilon_\infty + (\epsilon - \epsilon_\infty) \sum_k \frac{g_k}{1 + \omega^2\tau_k^2} \tag{4}$$

Once the fast dielectric constant has been defined with the above considerations, the nonequilibrium problem can be tackled. Despite the apparent simplicity of the two-component model, different approaches leading to different physical pictures exist and are still used. In the so-called Pekar partition the optical and the equilibrium polarizations are respectively proportional to

$$\frac{n^2 - 1}{n^2}, \qquad \frac{\epsilon - 1}{\epsilon} \tag{5}$$

so that their ratio is

$$\frac{n^2 - 1}{\epsilon - 1}\frac{\epsilon}{n^2}$$

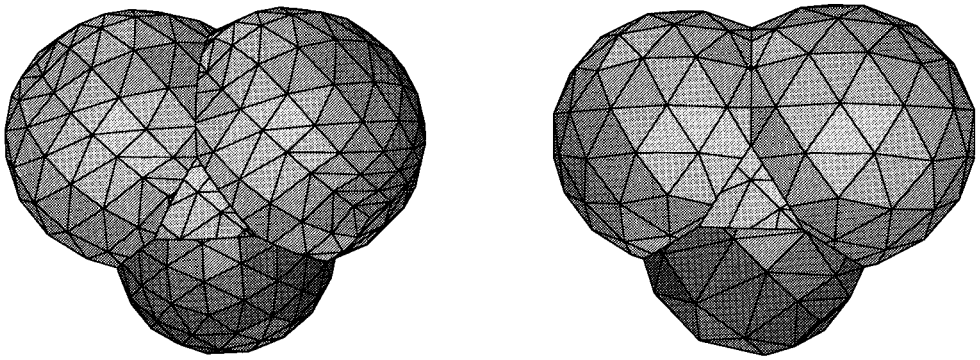

Figure 2. GEPOL cavities for acetone (hydrogen atoms are inserted in the same spheres as carbon atoms) covered by tesserae of area of 0.4 and 0.2 Å^2, respectively.

In water ($\epsilon = 78.4$, $n^2 = 1.75$) this means that about 45% of the solvent polarization is of electronic origin. On the other hand, some authors[48,49] pointed out that, taking into account a cross-term expressing the mutual influence between the electronic and the nuclear polarization, the contribution from the electronic source is markedly smaller, and it tends to become negligible in the limit of very high dielectric constant; very recently a similar model has been applied also by Truhlar and co-workers.[50] As shown in the following, our model belongs to this latter approach.

In the last section, we present some examples referred to very fast processes in solution, when $\epsilon_f = n^2$: the application to slower processes, e.g., molecular vibrations, is completely analogous, provided the proper ϵ_f is defined, but requires more technical considerations about the definition of the solute cavity, and it will be presented in a forthcoming paper.

2. PCM Solvation

In PCM the solute molecule is inserted in a cavity, formed by interlocking spheres centered on atoms or atomic groups:[51,52] the cavity surface is partitioned into small domains, called "tesserae", used to compute the surface integrals as finite sums (see Figure 2). The solvent polarization is described by means of a set of apparent charges $\{q_i\}$ placed in the surface tesserae, determined by the general equation

$$\mathbf{Dq} = -\mathbf{b} \tag{6}$$

where vector **q** collects the apparent solvation charges, vector **b** contains the solute electrostatic potential or the solute normal electric field on the cavity surface, and square matrix **D** depends on the cavity shape and on the solute dielectric constant as detailed below.

Three different PCM formalisms are currently used,[15] based on different physical models and mathematical treatments: they are referred to as D-PCM (dielectric version, based on the original formulation proposed in 1981),[12,24] C-PCM (conductor, based on the approach proposed by Klamt and Schüürmann in 1993[7] and implemented by Cossi and Barone[13]), and IEF-PCM (integral equation formalism, based on the mathematical treatment introduced by Cancès and Mennucci in 1997). Since it is relevant in the following, we report **D** and **b** elements explicitly for the three PCM versions.

In D-PCM

$$D_{ii} = \frac{1}{a_i}\left[\frac{4\pi}{\epsilon - 1} + 2\pi\left(1 + \sqrt{\frac{a_i}{4\pi R_i}}\right)\right]$$

$$D_{ij} = \frac{\vec{r}_i - \vec{r}_j}{|r_i - r_j|}\hat{n}_i$$

$$b_i = \vec{E}(\vec{r}_i)\cdot\hat{n}_i \tag{7}$$

In C-PDM

$$D_{ii} = \frac{\epsilon}{\epsilon - 1}\,1.07\sqrt{\frac{4\pi}{a_i}}$$

$$D_{ij} = \frac{\epsilon}{\epsilon - 1}\,\frac{1}{|r_i - r_j|}$$

$$b_i = V(\vec{r}_i) \tag{8}$$

In IEF-PCM

$$\mathbf{D} = \left(\frac{1}{2}\mathbf{I} - \tilde{\mathbf{D}}\right)^{-1}\left(\frac{\epsilon + 1}{2(\epsilon - 1)}\mathbf{I} - \tilde{\mathbf{D}}\right)\mathbf{S}$$

$$S_{ii} = 1.07\sqrt{\frac{4\pi}{a_i}}$$

$$S_{ij} = \frac{1}{|r_i - r_j|}$$

$$\tilde{D}_{ii} = \frac{S_{ii}}{2R_i}$$

$$\tilde{D}_{ij} = \frac{(\vec{r}_i - \vec{r}_j)\cdot\hat{n}_j}{|r_i - r_j|^3}$$

$$b_i = V(\vec{r}_i) \tag{9}$$

where a_i is the area of tessera i, $\vec{r}_i$ is the position of its center (defined as the average of the vertices), $\hat{n}_i$ is the unit vector normal to the surface in the ith tessera, R_i is the radius of the sphere to which the tessera belongs, ϵ is the solvent dielectric constant, and **I** is the unit matrix. Note that in eq 7, referred to D-PCM, the diagonal element D_{ii} is written in a form slightly different from that usually adopted:[53] in Appendix A this difference is discussed, showing that expression 7 is equivalent to the usual one for equilibrium solvation, while it is more suited to nonequilibrium calculations.

Once solvation charges have been defined through eq 6, they are used to correct the solute Hamiltonian

$$\hat{H} = \hat{H}^0 + V_\sigma \tag{10}$$

$$V_\sigma(\vec{r}) = \sum_i^{\text{tesserae}} \frac{q_i}{|r_i - r|} \tag{11}$$

$\hat{H}^0$ is the Hamiltonian for the solute in vacuo.

Since the solute wave function is modified by the solvation charges, which in turn depend on the solute electronic distribution, the charges and the wave function must be determined self-consistently: very effective procedures have been elaborated to do that for a large number of chemical systems in solution. It can be shown that the variational minimization with Hamiltonian 10 leads to the quantity (having the status of a free energy)

$$G = \left\langle \Psi \middle| \hat{H}^0 + \frac{1}{2}\hat{V}_\sigma \middle| \Psi \right\rangle = \langle \Psi | \hat{H}^0 | \Psi \rangle + \frac{1}{2}\sum_i q_i \left\langle \Psi \middle| \frac{1}{r - r_i} \middle| \Psi \right\rangle \tag{12}$$

Now, let us consider a sudden change in the electronic distribution (for example a photon absorption or emission), so that the solute wave function changes from $\Psi^{(1)}$ to $\Psi^{(2)}$. Before such a transition one can compute equilibrium solvation charges $\{q_i^{(1)}\}$, where index (1) indicates the electronic state to which the charges are equilibrated. If we split them into fast and slow components with the technique illustrated in the next section, we obtain

$$q_i = q_{i,\text{f}} + q_{i,\text{s}} \tag{13}$$

$$G_{\text{eq}}^{(1)} = \langle \Psi^{(1)} | \hat{H}^0 | \Psi^{(1)} \rangle + \frac{1}{2}\sum_i q_{i,\text{f}}^{(1)} V_i^{(1)} + \frac{1}{2}\sum_i q_{i,\text{s}}^{(1)} V_i^{(1)} \tag{14}$$

$$V_i^{(1)} = \left\langle \Psi^{(1)} \middle| \frac{1}{r - r_i} \middle| \Psi^{(1)} \right\rangle \tag{15}$$

where V_i is the electrostatic potential due to the solute on tessera i.

After the transition the fast component of solvation charges will be in equilibrium with the new wave function $\Psi^{(2)}$, whereas the slow charges are the same as in eq 14; of course, both sets of charges perturb the solute wave function. The free energy is

$$G_{\text{noneq}}^{(2)} = \langle \Psi^{(2)} | \hat{H}^0 | \Psi^{(2)} \rangle + \frac{1}{2}\sum_i q_{i,\text{f}}^{(2)} V_i^{(2)} + \frac{1}{2}\sum_{ij} \frac{q_{i,\text{f}}^{(2)} q_{j,\text{s}}^{(1)}}{r_i - r_j} + \sum_i q_{i,\text{s}}^{(1)} V_i^{(2)} \tag{16}$$

The last two terms in eq 16 express the interaction between the slow and the fast charges and between the slow charges and the solute (in state (2)), respectively. The factor 1/2 is dropped in the last term because now the $\mathbf{q}_\text{s}$'s are not self-consistent with the solute: in other words, no work has been spent in state (2) to create the slow charges. However, as clearly pointed out, e.g., in ref 29, to compare $G_{\text{noneq}}^{(2)}$ and $G_{\text{eq}}^{(1)}$ properly it is necessary to take into account the charging work spent in state (1) to create the $\mathbf{q}_\text{s}$'s: this work is equal to half the interaction of the slow charges with the solute and the fast charges, so that the expression for $G_{\text{noneq}}^{(2)}$ becomes

$$G_{\text{noneq}}^{(2)} = \langle \Psi^{(2)} | \hat{H}^0 | \Psi^{(2)} \rangle + \frac{1}{2}\sum_i q_{i,\text{f}}^{(2)} V_i^{(2)} + \frac{1}{2}\left(\sum_{ij} \frac{q_{i,\text{f}}^{(2)} q_{j,\text{s}}^{(1)}}{r_i - r_j} - \sum_{ij} \frac{q_{i,\text{f}}^{(1)} q_{j,\text{s}}^{(1)}}{r_i - r_j} \right) + \left(\sum_i q_{i,\text{s}}^{(1)} V_i^{(2)} - \frac{1}{2}\sum_i q_{i,\text{s}}{}^{(1)} V_i^{(1)} \right) \tag{17}$$

3. Fast and Slow Solvation Components

Now we consider the problem of splitting the solvation charges into fast and slow components: in the state $\Psi^{(1)}$ we must solve the two following equations at one time:

$$\mathbf{D}(\epsilon)\mathbf{q} = -\mathbf{b} \tag{18}$$

$$\mathbf{D}(\epsilon_\text{f})\mathbf{q}_\text{f} = -(\mathbf{b} + \mathbf{b}_\text{s}) \tag{19}$$

Equation 18 is simply eq 6, with the explicit indication of the dependence on the static dielectric constant. In eq 19 the fast dielectric constant ϵ_f is used instead of ϵ in the expression of $\mathbf{D}$; the term $\mathbf{b}_\text{s}$ represents the potential, or the normal component of the electric field, generated by the slow charges, and it expresses the relationship between fast and slow solvation charges. Note that the difference between the Pekar approach adopted by Bayliss, McRae, and many others and the present one lies in the cross-term $\mathbf{b}_\text{s}$ added in eq 19. The physical grounds for taking into account the mutual influence between the solvent electronic and nuclear polarization have been pointed out by Marcus:[21] from a different point of view, they have been discussed also by Brady and Carr[48] and reconsidered by Klamt.[49] In short, it can be shown that, following the Pekar partition, in the limit of very polar solvents ($\epsilon \rightarrow \infty$) the *orientational* contribution to the solvent polarization depends on the *optical* dielectric constant only, which is clearly counterintuitive (one would expect, on the contrary, that in this limit the effect of the optical polarization becomes negligible). Furthermore, introducing the cross-term $\mathbf{b}_\text{s}$ in eq 19 is equivalent to considering the solvent dielectric susceptibility $\chi = (\epsilon - 1)/4\pi$ as the linear combination of two components

$$\chi_\text{f} = (\epsilon_\text{f} - 1)/4\pi \tag{20}$$

and

$$\chi_\text{s} = \chi - \chi_\text{f} = (\epsilon - \epsilon_\text{f})/4\pi \tag{21}$$

which is also consistent with the phenomenological theory of frequency-dependent dielectric polarization.[45]

To solve system (18, 19) we introduce two matrix operators, Ω_V and Ω_E, expressing the electrostatic potential and the normal component of the electric field generated by a set of point charges on the cavity surface:

$$\Omega_V \mathbf{q}_x = \mathbf{V}_x$$
$$\Omega_E \mathbf{q}_x = \mathbf{E}_{n,x} \qquad x = \text{f, s} \tag{22}$$

$$(\Omega_V)_{ii} = 1.07\sqrt{\frac{4\pi}{a_i}}$$

$$(\Omega_V)_{ij} = \frac{1}{|r_i - r_j|} \tag{23}$$

$$(\Omega_E)_{ii} = \frac{1}{a_i} 2\pi \left(1 + \sqrt{\frac{a_i}{4\pi R_i}}\right)$$

$$(\Omega_E)_{ij} = \frac{(\vec{r}_i - \vec{r}_j)\cdot\hat{n}_i}{|r_i - r_j|} \qquad (24)$$

where all the quantities have the same meaning as in eq 7−9. The diagonal elements $(\Omega_V)_{ii}$ and $(\Omega_E)_{ii}$ express the potential and the normal electric field created by a charge density q_i/a_i on itself: their form can be found by the arguments reported in refs 7 and 24, respectively.

Then eq 19 becomes

$$\mathbf{D}(\epsilon_f)\mathbf{q}_f = -(\mathbf{b} + \Omega\mathbf{q}_s) = -\mathbf{b} - \Omega(\mathbf{q} - \mathbf{q}_f) \qquad (25)$$

where we put Ω generally (it becomes Ω_E in D-PCM and Ω_V in C-PCM and IEF-PCM). Recalling eq 18 and rearranging, we get

$$[\mathbf{D}(\epsilon_f) - \Omega]\mathbf{q}_f = [\mathbf{D}(\epsilon) - \Omega]\mathbf{q} \qquad (26)$$

$$\mathbf{q}_f = [\mathbf{D}(\epsilon_f) - \Omega]^{-1}[\mathbf{D}(\epsilon) - \Omega]\mathbf{q} \qquad (27)$$

$$\mathbf{q}_s = \mathbf{q} - \mathbf{q}_f \qquad (28)$$

Equations 27 and 28 are valid for all the PCM versions and allow one to split the solvation charges into slow and fast components. By substituting the explicit expressions for **D** and Ω, a very simple result is obtained for all the PCM versions:

$$\mathbf{q}_f = \frac{\epsilon_f - 1}{\epsilon - 1}\mathbf{q} \qquad (29)$$

$$\mathbf{q}_s = \frac{\epsilon - \epsilon_f}{\epsilon - 1}\mathbf{q} \qquad (30)$$

In Appendix B, eqs 29 and 30 are explicitly derived from eqs 27 and 28 for D-, C-, and IEF-PCM.

We note that eqs 29 and 30 correspond to the result found with different considerations by Klamt for COSMO[49] (analogous to C-PCM). The present treatment is more general and shows that this result holds for all the continuum models (provided that the cross-term in eq 19 is taken into account). Furthermore, from eqs 29 and 30 the ratio between the fast (slow) and the total solvation charges can be written in terms of the fast (slow) dielectric susceptibilities as

$$\frac{\mathbf{q}_x}{\mathbf{q}} = \frac{\chi_x}{\chi} \qquad x = \text{f, s} \qquad (31)$$

resembling Brady and Carr's equations, obtained by a completely different approach.

The above treatment refers to finite solvation charges computed in nonequilibrium conditions. On the other hand, in many applications one needs to consider the derivatives of the free energy in solution, or of the molecular Fock operator, with respect to some parameter λ (nuclear positions, external field components, etc.). Suitable algorithms have been elaborated to compute PCM contributions in geometry optimizations, force constant calculations, and interactions with electric and magnetic fields: such contributions depend on quantities related to the solvation charge derivatives, $\mathbf{q}^\lambda = \partial\mathbf{q}/\partial\lambda$, though the actual expressions are very compact and in general avoid the explicit use of $\mathbf{q}^\lambda$. Anyway, we shall examine briefly how $\mathbf{q}^\lambda$ has to be computed in nonequilibrium conditions, deferring more accurate analyses to further, specific works.

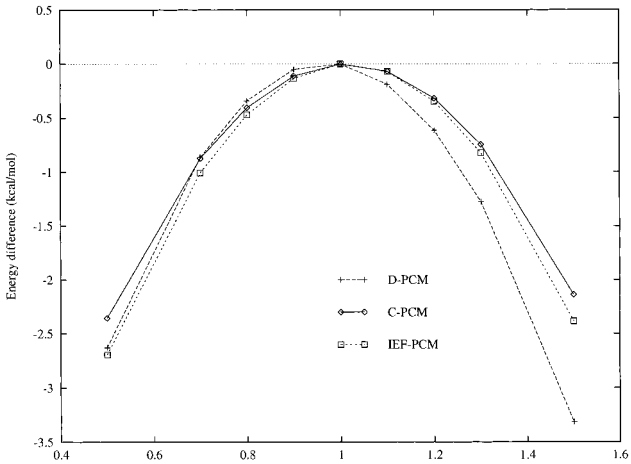

Figure 3. Energy difference (kcal/mol) in process 33 using different fast/slow partitions (eq 34).

When dynamical processes are considered, the speed of the variation of λ is of crucial importance. If this variation is associated to a very slow process, equilibrium solvation can be used to compute $\mathbf{q}^\lambda$: this is the case, for example, of geometry optimizations, which follow the potential energy surfaces and can be thought to be infinitely slow. If, otherwise, the frequency ω associated to the change of λ is high enough, a fast dielectric constant ϵ_f can be defined as above: this happens, for example, when one deals with solute nuclear vibrations or interactions with external fields. In this case only the fast component changes following λ, so that $\mathbf{q}^\lambda = \mathbf{q}_f^\lambda$. Recalling eq 19, we obtain

$$\mathbf{q}^\lambda = -\frac{\partial}{\partial\lambda}\{\mathbf{D}^{-1}(\epsilon_f)[\mathbf{b} + \mathbf{b}_s]\} = -\mathbf{D}^{-1}(\epsilon_f)\mathbf{b}^\lambda \qquad (32)$$

In eq 32 neither $\mathbf{b}_s$ nor **D** is affected by the derivative, since the slow charges are fixed by hypothesis and the size of the cavity is related to the distribution of solvent molecules around the solute, and we can assume that it changes only in equilibrium (slow) processes. Note that the independence of $\mathbf{q}^\lambda$ from $\mathbf{b}_s$ implies that the same expression could be obtained in the Pekar approach; moreover, formulations physically analogous to eq 32 have been already used to compute (hyper)polarizabilities in solution and to add solvent terms to time-dependent HF expressions.

4. Examples of Applications

The fast/slow partition of eqs 29 and 30 can be simply tested by imagining an excitation−deexcitation process

$$\text{state 1} \xrightarrow{h\nu} \text{some intermediate state} \xrightarrow{-h\nu} \text{state 1} \qquad (33)$$

so fast that the orientational component of the solvent polarization and the solute nuclear geometry do not change during the whole process. Of course one expects the energy computed at the beginning and at the end to be the same. We applied this imaginary process to H_2CO in chloroform ($\epsilon = 4.9$, $n^2 = 2.085$): first, the energy was computed at the Hartree−Fock level with 6-31G(d,p) basis set and with D-, C-, and IEF-PCM models. Then the solvation charges **q** obtained in this calculation were split into fast and slow components according to

$$\mathbf{q}_f = \lambda\frac{n^2 - 1}{\epsilon - 1}\mathbf{q}; \quad \mathbf{q}_s = \mathbf{q} - \mathbf{q}_f \qquad (34)$$

TABLE 2: H_2NO Ground State Geometrical Parameters (Å and deg) Optimized in Different Environments at the CAS(7,5)/6-31G(d) Level (the System Is Always Kept Planar)

	vacuum	benzene	CH_2Cl_2	DCE	acetone	methanol	water
r_{NO}	1.2986	1.2988	1.2988	1.2988	1.2990	1.2994	1.2995
r_{NH}	0.9949	0.9956	0.9974	0.9974	0.9980	0.9997	1.0023
∠(HNH)	118.82	118.96	118.96	118.97	118.99	118.99	119.03

Our model (eqs 29 and 30) corresponds to $\lambda = 1$, while the Pekar partition (eq 5) would correspond to $\lambda = \epsilon/n^2 = 2.35$. The energy at the end of process 33 was computed with eq 17 (in this case of course state (2) is the same as state (1)) using the slow charges $\mathbf{q}_s(\lambda)$ as given by eq 34. In Figure 3 we report the difference of energy before and after process 33 for different values of λ: one can see that when the mutual influence between fast and slow polarizations is accounted for, only the fast/slow partition proposed in the previous section ($\lambda = 1$) is able to give the same energy in the two calculations. With more polar solvents, we found larger and larger errors for $\lambda \neq 1$.

The next example is referred to the solvatochromic effect on H_2NO radical $n \rightarrow \pi^*$ electronic transition. Recently nitrosyl residues have been the object of many experimental and theoretical investigations, mainly for their usefulness in the study of magnetic and electronic properties of complex biochemical systems. Indeed, since nitrosyl spectroscopic and spin properties are very dependent on the local environment, such residues with suitable side chains can be used to probe the structure (and sometimes the dynamics) of micelles or membranes to which they are bonded. One of the properties used for this purpose is the UV spectrum in the region corresponding to nitrosyl $n \rightarrow \pi^*$ absorption: it is clearly very important to know accurately how the environment influences this transition energy. Of course, as illustrated in ref 30 for the case of acetone $S_0 \rightarrow S_1$ transition, one can compare calculated and experimental solvatochromic effects only if a number of features (such as nonelectrostatic interactions and discrete solvent molecule effects) are properly accounted for. However, in the present example we wish only to show the relative weight of nonequilibrium electrostatic interactions.

The calculations have been performed with 6-31G(d) basis set at the complete active space (CAS-SCF) level including seven electrons and five orbitals in the active space, using the program recently implemented in the Gaussian99 (development version) package,[54] which allows for CAS-SCF calculations with PCM.[20] The size of the spheres forming the cavity was determined by a procedure based on the solute topology,[52] which proved very effective in reproducing hydration free energies for many chemical systems.

The ground state geometry was optimized at the CAS(7,5) level in vacuo and in benzene, dichloromethane, 1,2-dichloroethane (DCE), acetone, methanol, and water, with the results reported in Table 2. In all the environments the molecule was kept planar, though it is known that the real minimum is slightly bent, because the inversion barrier is so low that the first vibrational eigenstate lies above it, and it is preferable to use the planar conformation as reference, as shown, e.g., in ref 55. In general the solvent has little effect on the geometrical parameters, the most conspicuous change being in the NO bond length.

The $n \rightarrow \pi^*$ transition energy was computed in vacuo ($\Delta E_{S_0 \rightarrow S_1} = 2.332$ eV $= 18\,810$ cm^{-1}) and in all the solvents at the corresponding ground state geometries. The PCM calculations were performed with both equilibrium (eq 14 for S_0 and S_1 energies) and nonequilibrium (eq 17 for S_1) solvation using the techniques described above. The solvent shifts, i.e., the differences between the transition energies in solution and in vacuo, are reported in Figure 4: it is evident that in polar environments nonequilibrium effects are very important and cannot be neglected at all.

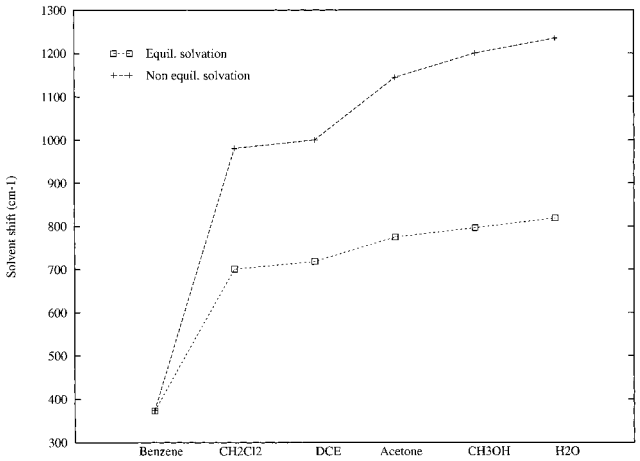

Figure 4. Solvent shift (cm^{-1}) for H_2NO $n \rightarrow \pi^*$ transition using equilibrium and nonequilibrium solvation in different solvents.

TABLE 3: H_2CO Geometrical Parameters (Å and deg) Optimized for the Ground State and for the First Excited Singlet ($n \rightarrow \pi^*$) at the CAS(6,4)/6-31G(d) Level in Water (Equilibrium Solvation in Both Cases)

	S_0	S_1
r_{CO}	1.2067	1.3521
r_{CH}	1.0870	1.0787
∠(HCH)	116.98	118.22
θ (out of plane)	0.00	40.29

Now we consider how an energy profile can be drawn taking into account the finite relaxation time of the surrounding solvent. For example, an electronic transition from the ground to the excited state can be seen as composed of two steps: a vertical transition in which the nuclear geometry remains frozen as in the excited state minimum. As for the solvent polarization, the fast component adjusts itself immediately to the wave function change, whereas the slow component relaxes together with the nuclear geometry. Indicating with $\mathbf{r}^{(1)}$, $\mathbf{r}^{(2)}$ the set of internal coordinates describing the ground and the excited state minima, respectively, the process can be sketched as

$$\Psi^{(1)}, \mathbf{r}^{(1)}, \mathbf{q}_f^{(1)}, \mathbf{q}_s^{(1)} \xrightarrow{\text{vert trans}} \Psi^{(2)}, \mathbf{r}^{(1)}, \mathbf{q}_f^{(2)}, \mathbf{q}_s^{(1)} \xrightarrow{\text{relax.}} \Psi^{(2)}, \mathbf{r}^{(2)}, \mathbf{q}_f^{(2)}, \mathbf{q}_s^{(2)} \quad (35)$$

We reproduced this process in the case of $S_0 \rightarrow S_1(n \rightarrow \pi^*)$ transition of formaldehyde in water: we computed S_0 and S_1 structures and energies at the CAS-SCF level with 6-31G(d,p) basis set, including in the active space six electrons and 4 orbitals; the calculations in water were performed with the C-PCM model.

In Table 3 the optimized geometries are reported for S_0 and S_1 in vacuo and in solution. As one can see, the most important difference involves the carbon atom pyramidalization (i.e., the out-of-plane angle of the oxygen with respect to the other three atoms): while in the ground state the molecule is planar, in S_1 the minimum corresponds to a strongly bent structure.

Then we choose the out-of-plane angle θ as the leading coordinate for the excited state geometry relaxation: the corresponding energy profiles in vacuo and in solution are reported in Figure 5 (for each value of θ the other coordinates were optimized). Different curves can be drawn in solution: one

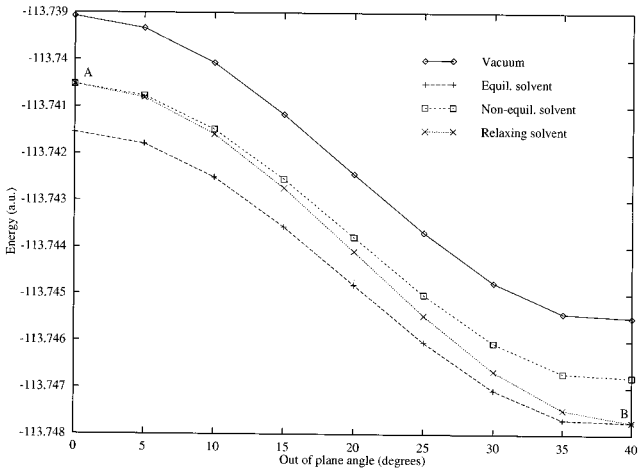

Figure 5. H_2CO S_1 energy (au) with respect to the out-of-plane angle in vacuo and in water, using equilibrium, nonequilibrium, and relaxing solvation.

corresponds to fully equilibrated solvent, i.e., for each geometry both $\mathbf{q}_f$ and $\mathbf{q}_s$ are adjusted to the excited state wave function. Another curve represents nonequilibrium solvation: in each point the $\mathbf{q}_f$ are in equilibrium with the excited state but the $\mathbf{q}_s$ are generated by the corresponding ground state wave function. Of course, neither the former nor the latter curve represents a relaxation process in which the solvent rearranges at a speed comparable to that of the solute: for $\theta = 0$ the solvent is not equilibrated (point A in Figure 5) whereas at the end of the relaxation process also the solvent is expected to be fully equilibrated (point B in Figure 5).

We propose to use the energy profile corresponding to the "relaxing solvent" line in Figure 5: the energies for each θ can be computed by allowing the $\mathbf{q}_s$ to go from the nonequilibrium to the equilibrium arrangement during the geometry optimization. We assume that the nuclear motions involved in solute and in solvent rearrangement are similar and proceed at the same speed: then the $\mathbf{q}_s$ relax exponentially as

$$\mathbf{q}_s(\theta) = \mathbf{q}_s^A \exp\left\{-\frac{\theta-\theta_1}{\theta_2-\theta_1}(\ln \mathbf{q}_s^A - \ln \mathbf{q}_s^B)\right\} \qquad (36)$$

$$\theta_1 = 0°; \qquad \theta_2 = 40.29°$$

where $\mathbf{q}_s^A$ are the nonequilibrium slow charges for $\theta = 0°$ and $\mathbf{q}_s^B$ the equilibrium slow charges for $\theta = 40.29°$; in each point the free energy in solution was computed with eq 17. This example shows that an effective treatment of nonequilibrium solvation can help in drawing physically correct energy profiles in solution.

5. Conclusions

In the past decade continuum solvation models have proven very useful to describe solute−solvent interactions at quantum high level. In the effort to extend the applicability of such models also to dynamical processes in solution, great attention must be paid to nonequilibrium effects, which arise when the time scale of the studied processes is comparable with the relaxation time of the solvent polarization.

In the present work we report on a part of the methodological grounds needed for the quantum description of dynamics in solution, a field which, in our opinion, will receive more and more attention in the near future. We have shown how the PCM, a well-known, effective, and reliable continuum solvation model, can be used to describe nonequilibrium effects, for processes with any characteristic frequency. The key feature of the present approach is the definition of fast and slow solvation charges, the former always equilibrated to the solute, the latter delayed or fixed; of course the extent of such a partition depends on the frequency of the considered perturbation.

Unlike other nonequilibrium PCM descriptions, the present one can be applied to all the variants of the method (in fact, this fast/slow partition is general for any ASC method), and the partition is particularly simple and effective. The procedure has been implemented in the development version of the Gaussian package, and some tests have been reported and discussed, to illustrate some of the possible applications. Of course the chemical interest for such a technique is very wide, ranging from the study of electronic transitions and vibrational motions to the description of proton transfer reactions and time-resolved geometry relaxations.

Appendix A

In D-PCM we use for the **D** matrix diagonal element the expression (eq 7)

$$D_{ii} = \frac{1}{a_i}\left[\frac{4\pi}{\epsilon-1} + 2\pi(1+\eta_i)\right], \quad \eta_i = \sqrt{\frac{a_i}{4\pi R_i}} \qquad (37)$$

instead of the usual form[53]

$$D_{ii} = \frac{1}{a_i}\left[\frac{4\pi\epsilon}{\epsilon-1} - 2\pi(1-\eta_i)\right] \qquad (38)$$

One can easily verify that these expressions are identical, provided the value of ϵ is the same at the numerator and at the denominator of eq 38. The quantity $4\pi/(\epsilon - 1)$ expresses the proportionality between the solvation charges and the normal field on the outer side of the surface; the ϵ at the numerator of eq 38 appears when the field is taken inside the cavity, according to

$$(E_n)_{i,\text{in}} = \epsilon(E_n)_{i,\text{out}} \qquad (39)$$

where $(E_n)_i$ is the normal component of the electric field in tessera i.

Then the solvation charge q_i is

$$q_i = -\frac{\epsilon-1}{4\pi}(E_n)_{i,\text{out}} = -\frac{\epsilon-1}{4\pi\epsilon}(E_n)_{i,\text{in}} \qquad (40)$$

In terms of the quantities defined above we have

$$q_i = -\frac{1}{a_i}\frac{\epsilon-1}{4\pi}\left[b_i + 2\pi(1+\eta_i)q_i + \sum_{j\neq i} a_i \frac{(\vec{r}_i - \vec{r}_j)\cdot\hat{n}_i}{|r_i - r_j|^3} q_j\right] \quad \text{outside} \qquad (41)$$

$$q_i = -\frac{1}{a_i}\frac{\epsilon-1}{4\pi\epsilon}\left[b_i - 2\pi(1-\eta_i)q_i + \sum_{j\neq i} a_i \frac{(\vec{r}_i - \vec{r}_j)\cdot\hat{n}_i}{|r_i - r_j|^3} q_j\right] \quad \text{inside} \qquad (42)$$

We recall that b_i is the normal component of the solute electric field, and that the last term in the right-hand side of eqs 41 and 42 is the contribution from the other solvation charges: these two terms do not meet any discontinuity crossing the surface. On the other hand, $\pm 2\pi(1 \pm \eta_i)(q_i/a_i)$ is called the self-

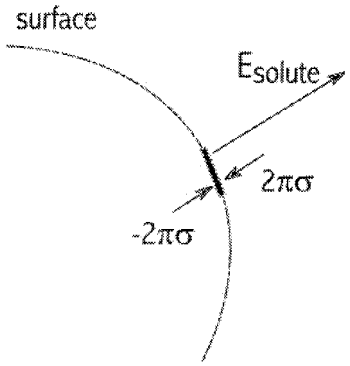

Figure 6. Effect of electric field created by surface charge density σ.

polarization term and it expresses the normal field created by the charge density q_i/a_i on itself; this contribution is the source of the electric field discontinuity across the surface. In the case of a planar surface the self-polarization field is $-2\pi(q_i/a_i)$ inside the cavity and $+2\pi(q_i/a_i)$ outside. As shown in Figure 6, its effect is to strengthen the field inside the cavity and to weaken it outside. As our cavities are not planar but spherical, a correction $\eta_i = (a_i/4\pi R_i)^{1/2}$ is added to take into account the curvature effect; this correction has a positive sign for concave surfaces (outside the cavity) and a negative sign for convex surfaces (inside).

Traditionally eq 38 (field inside the cavity) is used in D-PCM: however in the case of nonequilibrium solvation it cannot be used because the relationship

$$(E_n)_{i,\text{in}} = \epsilon(E_n)_{i,\text{out}}$$

holds only in the equilibrium case. If a part of the solvation charge density is not equilibrated to the solute, the field discontinuity is no longer proportional to ϵ: such a problem can be avoided by using eq 37 (field outside the cavity). In equilibrium conditions the two approaches are perfectly equivalent; on the other hand, only eq 37 is able to provide the correct result in nonequilibrium calculations (for example in the excitation−deexcitation process considered at the beginning of section 4). Then, to avoid confusion, we propose to adopt eq 37 for all the D-PCM calculations, both in the equilibrium case and in the nonequilibrium case.

Appendix B

C-PCM. This is the simplest case. Recalling eqs 8 and 23, it is clear that

$$\mathbf{D}(\epsilon) = \frac{\epsilon}{\epsilon - 1}\Omega_V, \qquad \mathbf{D}(\epsilon_\text{f}) = \frac{\epsilon_\text{f}}{\epsilon_\text{f} - 1}\Omega_V \tag{43}$$

so that the general expressions 27 and 28 become

$$\mathbf{q}_\text{f} = \left[\frac{\epsilon_\text{f}}{\epsilon_\text{f} - 1}\Omega - \Omega\right]^{-1}\left[\frac{\epsilon}{\epsilon - 1}\Omega - \Omega\right]\mathbf{q} = \frac{\epsilon_\text{f} - 1}{\epsilon - 1}\mathbf{q} \tag{44}$$

$$\mathbf{q}_\text{s} = \mathbf{q} - \mathbf{q}_\text{f} = \frac{\epsilon - \epsilon_\text{f}}{\epsilon - 1}\mathbf{q} \tag{45}$$

D-PCM. Comparing eqs 7 and 24, one obtains

$$D_{ii}(\epsilon) - (\Omega_E)_{ii} = \frac{1}{a_i}\frac{4\pi}{\epsilon - 1} \tag{46}$$

$$D_{ij} - (\Omega_E)_{ij} = 0 \qquad \text{for any } i \neq j \tag{48}$$

$$D_{ii}(\epsilon_\text{f}) - (\Omega_E)_{ii} = \frac{1}{a_i}\frac{4\pi}{\epsilon_\text{f} - 1} \tag{47}$$

Then

$$[\mathbf{D}(x) - \Omega_E] = \frac{4\pi}{x - 1}\mathbf{A}{-}1 \qquad x = \epsilon, \epsilon_\text{f} \tag{49}$$

where **A** is a diagonal matrix collecting the areas of surface-tesserae.

Equations 27 and 28 become

$$\mathbf{q}_\text{f} = \left[\frac{4\pi}{\epsilon_\text{f} - 1}\mathbf{A}^{-1}\right]^{-1}\left[\frac{4\pi}{\epsilon - 1}\mathbf{A}^{-1}\right]\mathbf{q} = \frac{\epsilon_\text{f} - 1}{\epsilon - 1}\mathbf{q} \tag{50}$$

$$\mathbf{q}_\text{s} = \mathbf{q} - \mathbf{q}_\text{f} = \frac{\epsilon - \epsilon_\text{f}}{\epsilon - 1}\mathbf{q} \tag{51}$$

i.e., the same result as for C-PCM.

IEF-PCM. Comparing eqs 9 and 23, one can easily see that $\mathbf{S} = \Omega_V$, so that eq 27 becomes in this case

$$\mathbf{q}_\text{f} = \left[\left(\frac{1}{2}\mathbf{I} - \tilde{\mathbf{D}}\right)^{-1}\left(\frac{\epsilon_\text{f} + 1}{2(\epsilon_\text{f} - 1)}\mathbf{I} - \tilde{\mathbf{D}}\right)\Omega_V - \Omega_V\right]^{-1}\left[\left(\frac{1}{2}\mathbf{I} - \tilde{\mathbf{D}}\right)^{-1}\left(\frac{\epsilon + 1}{2(\epsilon - 1)}\mathbf{I} - \tilde{\mathbf{D}}\right)\Omega_V - \Omega_V\right]\mathbf{q} =$$

$$\Omega_V{}^{-1}\left[\left(\frac{1}{2}\mathbf{I} - \tilde{\mathbf{D}}\right)^{-1}\left(\frac{\epsilon_\text{f} + 1}{2(\epsilon_\text{f} - 1)}\mathbf{I} - \tilde{\mathbf{D}} - \frac{1}{2}\mathbf{I} + \tilde{\mathbf{D}}\right)\right]^{-1}\left[\left(\frac{1}{2}\mathbf{I} - \tilde{\mathbf{D}}\right)^{-1}\left(\frac{\epsilon + 1}{2(\epsilon - 1)}\mathbf{I} - \tilde{\mathbf{D}} - \frac{1}{2}\mathbf{I} + \tilde{\mathbf{D}}\right)\right]\Omega_V\mathbf{q} = \Omega_V{}^{-1}\left[\frac{1}{2}\left(\frac{\epsilon_\text{f} + 1}{\epsilon_\text{f} - 1} - 1\right)\mathbf{I}\right]^{-1}\left(\frac{1}{2}\mathbf{I} - \tilde{\mathbf{D}}\right)\left(\frac{1}{2}\mathbf{I} - \tilde{\mathbf{D}}\right)^{-1}\left[\frac{1}{2}\left(\frac{\epsilon + 1}{\epsilon - 1} - 1\right)\mathbf{I}\right]\Omega_V\mathbf{q} =$$

$$\Omega_V{}^{-1}\left(\frac{2}{\epsilon_\text{f} - 1}\right)^{-1}\left(\frac{2}{\epsilon - 1}\right)\Omega_V\mathbf{q} \tag{52}$$

$$\mathbf{q}_\text{f} = \frac{\epsilon_\text{f} - 1}{\epsilon - 1}\mathbf{q} \tag{53}$$

which corresponds once again to the result found for C- and D-PCM.

References and Notes

(1) Tomasi, J.; Persico, M. *Chem. Rev.* **1994**, *94*, 2027.
(2) Rivail, J. L.; Rinaldi, D.; Luiz-Lopez, M. F. *Liquid State Quantum Chemistry* in *Computational Chemistry: Review of Current Trends*; Lecszynski, J., Ed.; World Scientific: Singapore, 1995.
(3) Cramer, C. J.; Truhlar, D. G. In *Reviews in Computational Chemistry*; Lipkowitz, K. B., Boyd, D. B., Eds.; VCH: New York, 1995.
(4) Cramer, C. J.; Truhlar, D. G. *Chem. Rev.* **1999**, *99*, 2161.
(5) Rinaldi, D.; Rivail, L.; Rguini, N. *J. Comput. Chem.* **1992**, *13*, 675.
(6) Foresman, J. B.; Keith, T. A.; Wiberg, K. B.; Snoonian, J.; Frisch, M. J. *J. Phys. Chem.* **1996**, *100*, 16098.
(7) Klamt, A.; Schuurmann, G. *J. Chem. Soc., Perkin Trans. 2* **1993**, 799.
(8) Truong, T. N.; Stefanovich, E. V. *Chem. Phys. Lett.* **1995**, *240*, 253.
(9) Klamt, A.; Jonas, V.; Burger, T.; Lohrenz, J. C. W. *J. Phys. Chem. A* **1998**, *102*, 5074.
(10) Dillet, V.; Rinaldi, D.; Bertran, J.; Rivail, J. L. *J. Chem. Phys.* **1996**, *104*, 9437.
(11) Stefanovich, E. V.; Truong, T. N. *J. Chem. Phys.* **1996**, *105*, 2961.
(12) Cossi, M.; Barone, V.; Cammi, R.; Tomasi, J. *Chem. Phys. Lett.* **1996**, *255*, 327.
(13) Barone, V.; Cossi, M. *J. Phys. Chem. A* **1998**, *102*, 1995.

(14) Mennucci, B.; Cancès, E.; Tomasi, J. *J. Phys. Chem.* **1997**, *101*, 10506.
(15) Amovilli, C.; Barone, V.; Cammi, R.; Cancès, E.; Cossi, M.; Mennucci, B.; Pomelli, C. S.; Tomasi, J. *Adv. Quantum Chem.* **1998**, *32*, 227.
(16) Cossi, M.; Barone, V. *J. Chem. Phys.* **1998**, *109*, 6246.
(17) Mennucci, B.; Cammi, R.; Tomasi, J. *J. Chem. Phys.* **1999**, *110*, 6858.
(18) Tomasi, J.; Cammi, R.; Mennucci, B. *Int. J. Quantum Chem.* **1999**, *75*, 783.
(19) Cammi, R.; Mennucci, B. *J. Chem. Phys.* **1999**, *110*, 9877.
(20) Cossi, M.; Barone, V.; Robb, M. A. *J. Chem. Phys.* **1999**, *111*, 5295.
(21) Marcus, R. A. *J. Chem. Phys.* **1956**, *24*, 979.
(22) Kim, H. J.; Hynes, J. T. *J. Am. Chem. Soc.* **1992**, *114*, 10508; *J. Am. Chem. Soc.* **1992**, *114*, 10528.
(23) For a review of the bibliography related to this topic, see for instance ref 4 and references therein.
(24) Miertuš, S.; Scrocco, E.; Tomasi, J. *Chem. Phys.* **1981**, *55*, 117.
(25) Cammi, R.; Tomasi, J. *J. Comput. Chem.* **1995**, *16*, 1449.
(26) Bonaccorsi, R.; Cimiraglia, R.; Tomasi, J. *J. Comput. Chem.* **1983**, *4*, 567.
(27) Aguilar, M. A.; Olivares del Valle, F. J.; Tomasi, J. *J. Chem. Phys.* **1993**, *98*, 7375.
(28) Cammi, R.; Tomasi, J. *Int. J. Quantum Chem.: Quantum Chem. Symp.* **1995**, *29*, 465.
(29) Mennucci, B.; Cammi, R.; Tomasi, J. *J. Chem. Phys.* **1998**, *109*, 2798.
(30) Cossi, M.; Barone, V. *J. Chem. Phys.* **2000**, *112*, 2127.
(31) Lippert, E. *Z. Elektrochem.* **1957**, *61*, 952.
(32) Ooshika, Y. *J. Phys. Soc. Jpn.* **1954**, *9*, 594.
(33) Bayliss, N. S.; McRae, E. G. *J. Phys. Chem.* **1954**, *58*, 1002.
(34) McRae, E. G. *J. Phys. Chem.* **1957**, *61*, 562.
(35) Amos, A. T.; Burrows, B. L. *Adv. Quantum Chem.* **1973**, *7*, 289.
(36) Rao, C. N. R.; Singh, S.; Senthilnathan, V. P. *Chem. Soc. Rev.* **1976**, *5*, 297.
(37) Sánchez, M. L.; Aguilar, M. A.; Olivares del Valle, F. J. *J. Phys. Chem.* **1995**, *99*, 15758.
(38) Serrano-Andrés, L.; Fülscher, M. P.; Karlström, G. *Int. J. Quantum Chem.* **1997**, *65*, 167.
(39) Ågren, H.; Mikkelsen, K. V. *J. Mol. Struct. (THEOCHEM)* **1991**, *234*, 425.
(40) Karelson, M. M.; Zerner, M. C. *J. Phys. Chem.* **1992**, *96*, 6949.
(41) Marcus, R. A. *Faraday Symp. Chem. Soc.* **1975**, *10*, 60.
(42) Truhlar, D. G.; Schenter, G. K.; Garret, B. C. *J. Chem. Phys.* **1993**, *98*, 5756.
(43) Basilevsky, M. V.; Chudinov, G. E.; Napolov, D. V. *J. Phys. Chem.* **1993**, *97*, 3270.
(44) Kim, H. J.; Hynes, J. T. *J. Chem. Phys.* **1990**, *93*, 5194.
(45) Böttcher, C. J. F. *Theory of electric polarization*, 2nd ed.; Elsevier: New York, 1973; Vol. II.
(46) Hasted, J. B. In *Water: a comprehensive treatise*; Franks, F., Ed.; Plenum Press: New York, 1972; Vol. I.
(47) Dannhauser, W.; Cole, R. H. *J. Chem. Phys.* **1955**, *23*, 1762.
(48) Brady, J. E.; Carr, P. W. *J. Phys. Chem.* **1985**, *89*, 5759.
(49) Klamt, A. *J. Phys. Chem.* **1996**, *100*, 3349.
(50) Li, J.; Cramer, C. J.; Truhlar, D. G. *Int. J. Quantum Chem.* **2000**, *77*, 264.
(51) Pascual-Ahuir, J. L.; Silla, E.; Tunòn, I. *J. Comput. Chem.* **1994**, *15*, 1127.
(52) Barone, V.; Cossi, M.; Tomasi, J. *J. Chem. Phys.* **1997**, *107*, 3210.
(53) Cammi, R.; Tomasi, J. *J. Comput. Chem.* **1995**, *16*, 1449.
(54) M. J. Frisch, G. W. Trucks, H. B. Schlegel, G. E. Scuseria, M. A. Robb, J. R. Cheeseman, V. G. Zakrzewski, J. A. Montgomery, Jr., R. E. Stratmann, J. C. Burant, S. Dapprich, J. M. Millam, A. D. Daniels, K. N. Kudin, M. C. Strain, O. Farkas, J. Tomasi, V. Barone, M. Cossi, R. Cammi, B. Mennucci, C. Pomelli, C. Adamo, S. Clifford, J. Ochterski, G. A. Petersson, P. Y. Ayala, Q. Cui, K. Morokuma, D. K. Malick, Rabuck, A. D.; Raghavachari, K.; Foresman, J. B.; Ortiz, J. V.; Baboul, A. G.; Cioslowski, J.; Stefanov, B. B.; Liu, G.; Liashenko, A.; Piskorz, P.; Komaromi, I.; Gomperts, R.; Martin, R. L.; Fox, D. J.; Keith, T.; Al-Laham, M. A.; Peng, C. Y.; Nanayakkara, A.; Gonzalez, C.; Challacombe, M.; Gill, P. M. W.; Johnson, B.; Chen, W.; Wong, M. W.; Andres, J. L.; Gonzalez, C.; Head-Gordon, M.; Replogle, E. S.; Pople, J. A. *Gaussian99*, Development Version (Revision A.8+); Gaussian, Inc.: Pittsburgh, PA, 1998.
(55) Rega, N.; Cossi, M.; Barone, V. *J. Chem. Phys.* **1996**, *105*, 11060.